

Research article

Monitoring the trends in emissions from coal-fired power stations in Lephalale (Limpopo) during the 2010-2022 period using remotely sensed data

Zizipho Keli¹, Paidamwoyo Mhangara^{1*}, Lerato Shikwambana^{1,2}

¹School of Geography, Archaeology and Environmental Studies, University of the Witwatersrand, Johannesburg 2000, South Africa

²Earth Observation Directorate, South African National Space Agency, Pretoria 0001, South Africa

*Corresponding author: paida.mhangara@wits.ac.za

Received: 29 May 2024 - Reviewed: 5 November 2024 - Accepted: 15 November 2024

<https://doi.org/10.17159/caj/2024/34/2.18784>

Abstract

This study uses datasets from the Sentinel-5P, Modern Era Retrospective Analysis for Research and Applications, version 2 (MERRA-2), Ozone Monitoring Instrument (OMI) and Goddard Earth Observing System with Chemistry Model (GEOS-Chem) to investigate the spatial and temporal distribution of sulphur dioxide (SO₂), nitrogen dioxide (NO₂), carbon dioxide (CO₂) and carbon monoxide (CO) in the town of Lephalale, South Africa. Lephalale has two active coal-fired power stations which continuously releases SO₂, NO₂, CO₂ and CO. Within the 2010-2022 period of the study, it was found that SO₂ and NO₂ had the most significant trend of increase from 2010-2019, and decreased from 2020-2021 due to the COVID-19 global pandemic. CO₂ and CO kept a fluctuating trend between the 2010-2022 study period. The results of the study showed that the poor air quality in Lephalale is consequential of these emissions by coal combustion. Most importantly, if no mitigation measures are taken and strictly followed by coal mines and electricity generators, the lives of the people in and around Lephalale and Limpopo province will be severely affected.

Keywords

emission, Sentinel-5P, MERRA-2, air quality, coal-fired power station

Introduction

Global emissions from fossil fuel use, mainly coal combustion, have been one of the most significant causes of environmental and atmospheric damage, significantly impacting human health (Farzad et al., 2021). A notable amount of these emissions are greenhouse gasses (GHG) and particulate matter (both PM_{2.5} and PM₁₀) that are a result of the generation of electrical power (Duncan et al., 2014; Albers et al., 2015). In 2020, there were 18 coal-fired power stations in South Africa, all owned by Eskom, the country's sole electricity producer and generating over 80% of the national grid's electricity (Winning, 2021). With so many coal-fired power stations, Winning (2021) denotes that the country holds the 12th position in the world's list of greenhouse gas emitters. In addition, Shikwambana et al. (2020) noted that South Africa and other countries, including India and Brazil, were among the top 20 on the list of greenhouse gas emitters. Amongst these 18 coal power stations, a prominent number are in the Highveld region and thus serve as hotspots for the country's most significant greenhouse gas emissions (Shikwambana et al., 2020). One of these coal-fired power stations is located in the Waterberg-Bojanala Priority Area (WBPA) in the Limpopo province, outside the town of Lephalale.

The very first construction of the power station began in 2007, and according to Marcatelli (2020), it was to be completed in 2020. Still, its completion and full use were only a year after the estimated completion. The WBPA was initially designated as an air quality priority area due to the potential risks of future air pollution. It has since become a recognized air pollution hotspot. The primary sources of emissions in this area include mining, industry, residential activities, motor vehicles, and biomass burning (Wernecke et al., 2023).

GHG emissions caused by the complete and incomplete coal combustion for electricity generation have been a notable problem in South Africa and other global countries and promise to persist if there are no reductions to emissions and a shift to cleaner energy sources (Barnes et al., 2009; Jiang et al., 2022). Power stations worldwide have struggled to develop ameliorative measures to better the scourge of pollutants. This greatly affects communities near and around these coal-fired stations and, to a greater extent, the world. If not adequately mitigated, the combustion and subsequent gasses and particulate matter pose dangerous health risks to human health. These risks are significant and lead to morbidity and premature mortality

among the young and the old as they are more vulnerable to respiratory, brain and lung death-related illnesses (Gupta et al., 2006; Lelieveld et al., 2019). As significant as these are, research centred on the main study – the Medupi Power Station – is quite limited and does not give extensive evidence to account for the station's impact on air quality in surrounding communities.

Arowosegbe et al. (2022) and the World Health Organization's report of 2012 noted that 87% of the 3 million deaths that same year were due to air pollution in low and middle-income countries as these had higher air polluting emissions. Africa is no exception to these high rates as it is a less developed continent with few resources to rehabilitate and manage the environment repeatedly to reduce the effects over time. Reports urging for the transition from fossil fuel energy to clean, renewable energy sources have termed Algeria, Nigeria, Morocco, Egypt and South Africa as 'Africa's Big Five', as these five countries are the biggest consumers of fossil fuels, particularly coal, for energy generation (Mutezo and Mulopo, 2021). Furthermore, South Africa is regarded as the continent's biggest greenhouse gas emitter because it is the most industrialised country in Africa, which has put a toll on the atmospheric environment and people's lives (Shikwambana et al., 2020).

The objectives of this study are (1) to assess the long-term time-series trends of sulphur dioxide (SO₂), nitrogen dioxide (NO₂), carbon dioxide (CO₂) and carbon monoxide (CO) emissions in the Limpopo province for the period 2010 to 2022, (2) to map the spatial distribution of SO₂, NO₂, CO and CO₂ in the Limpopo province, and (3) to provide recommendation of the transitional shift from non-renewable to cleaner energy, thereby protecting the environment.

Study area

The province of Limpopo is located in the northern-east of South Africa (see Figure 1) and is the fifth biggest in the country. According to Köppen and Geiger, the province is classified as Cwc, as it is temperate with summer rainfall and hot summers

between October and April (Peel et al., 2007; Rapolaki et al., 2021). Lephalale (23.66°S, 27.74°E) is located northwest of the Limpopo province. It is found in the Waterberg-Bojanala Priority Area and is home to two power stations: the Medupi Power Station and the Matimba Power Station. A coal mine, Exxaro Groogeluk, provides coal to both power stations through a conveyor belt (Muthige, 2013). Unfortunately, Medupi and Matimba Power Stations are located in a rural location where most of the population is uneducated about their hazardous surroundings to the byproduct emissions in Lephalale (Shamuyarira & Gumbo, 2014)

Data and method

Sentinel-5P (Precursor)

The Sentinel-5 Precursor (Sentinel-5P) was developed by the European Space Agency (ESA) and launched on 13 October 2017 (Shami et al., 2022). The Tropospheric Monitoring Instrument (TROPOMI) is the instrument on board the Sentinel-5P satellite. Its role is to detect trace gasses using three streams: near-real-time (NRTI), offline (OFFL) and reprocessing (RPRO). TROPOMI has a spatial resolution of 3.5 × 7 km² and a swath width of 2600 km, allowing global atmospheric coverage (Shikwambana et al., 2020). In addition, it comprises a temporal resolution of less than a few hours, passing by an area and providing data on it twice a day (Theys et al., 2019). TROPOMI is made up of seven spectral bands being: ultraviolet (UV-1) (270-300 nm) and (UV-2) (300-370 nm), visible (VIS) (370-500 nm), near-infrared (NIR-1) (685-710 nm) and (NIR-2) (745-773 nm), shortwave (SWIR-1) (1590-1675 nm) and (SWIR-3) (2305-2385 nm) (Theys et al., 2019). Before and after its launch, its mission is to monitor ultraviolet (UV) radiation, the incidence of ozone (O₃) in the atmosphere, atmospheric air quality and climate. TROPOMI measurements include SO₂, NO₂, CO, O₃, CH₄ and formaldehyde (CH₂O) (Shami et al., 2022). More details on sentinel-5P are found in Theys et al. (2019), Tilstra et al. (2020) and Verhoelst et al. (2021). The data used in this study is between 2018 and 2022.

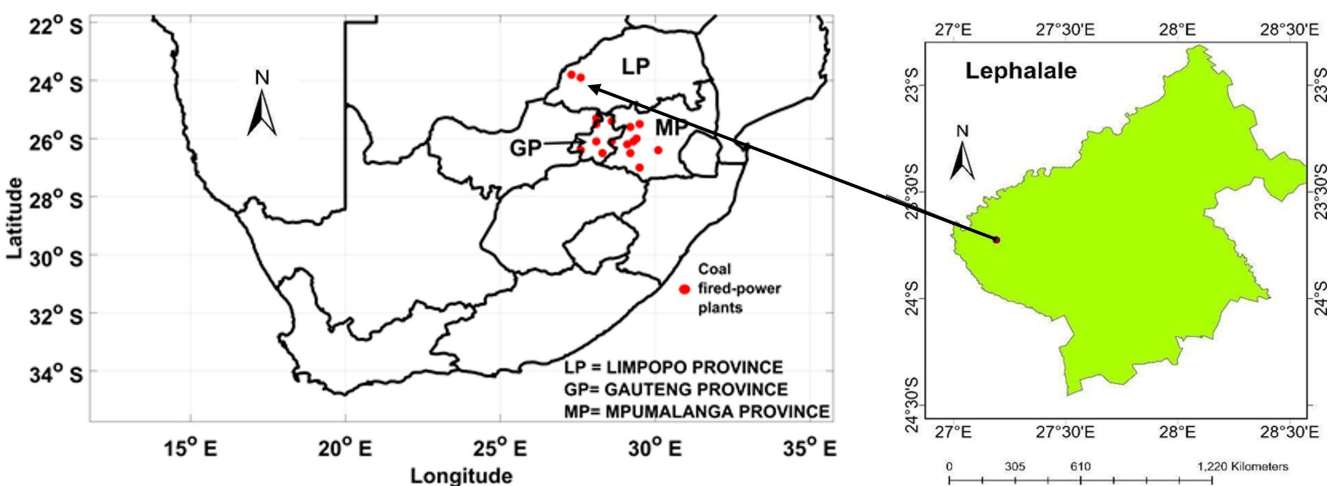


Figure 1: Map showing the coal-fired power stations that serve as SO₂, NO₂, CO and CO₂ emitters in Limpopo and South Africa

MERRA-2

Modern Era Retrospective Analysis for Research and Applications, version 2 (MERRA-2) is a reanalysis of the modern satellite era launched by NASA's Global Modeling and Assimilation Office (GMAO) on 1 January 1980. For its full function, it includes the Goddard Earth Observing System, version 5 (GEOS-5) and the Atmospheric Data Assimilation System (ADAS), version 5.12.4 satellites, and using these sustains GMAO's commitment to near-real-time (NRTI) climate analysis (Shikwambana et al., 2020). It can separate different aerosols from one another, especially GHGs, and measures surface temperature, air temperature and wind speed (Gelaro et al., 2017; Shikwambana et al., 2020). The MERRA-2 satellite uses a cubed-sphere latitude by longitude spectral resolution of $0.5^\circ \times 0.625^\circ$ and 72 hybrid-eta layers from the Earth's surface for configuration (Gelaro et al., 2017). More details on MERRA-2 can be found in Gelaro et al. (2017), Buchard et al. (2017) and Randles et al. (2017). The data used in this study is between 2018 and 2022.

OMI

The Ozone Monitoring Instrument (OMI) is a satellite instrument launched aboard the Earth Observing System (EOS) on 15 July 2004. It is driven by the European Global Ozone Monitoring Experiment (GOME) and the Scanning Imaging Absorption Spectrometer for Atmospheric Cartography (SCIAMACHY) (Levelt et al., 2006). It measures solar radiation that is reflected using spectral bands ultraviolet (UV-1) (270-310 nm), (UV-2) (310-365 nm) and visible (VIS) (365-500 nm) (Levelt et al., 2006). Through these spectral bands, this satellite sensor can measure trace aerosol gasses like SO_2 , NO_2 , HCHO, O_3 and UV radiance (Mokgoja et al., 2023). OMI has a spatial resolution of $13 \times 25 \text{ km}^2$ and a daily temporal resolution. More details on the OMI can be found in Boersma et al. (2002), Bucsele et al. (2006), Levelt et al. (2006), and Levelt et al. (2018). The data used in this study is between 2018 and 2022.

GEOS-Chem

The Goddard Earth Observing System with Chemistry Model (GEOS-Chem) is a global 3-D model of atmospheric chemistry driven by meteorological inputs. The model output is a set of quantities, such as tracer concentrations in every grid cell (Miatselskaya et al., 2022). The near-real-time GEOS Forward Processing (GEOS FP) output provides data globally at a horizontal resolution of $0.25^\circ \times 0.3125^\circ$ (Fritz et al., 2022). Bey et al. (2001) describe the standard application of the GEOS-Chem model. The data used in this study is between 2015 and 2021.

SQMK test

Sneyers first used the Sequential Mann-Kendall (SQMK) test in the 1990s to detect any change between a significant trend's starting and ending period (Sneyers, 1990). This test has two series of analyses, a progressive $u(t)$ and a retrograde $u'(t)$ series. With these, the test detects the beginning of a significant change and trend (Mosmann et al., 2004). More details on the SQMK test can be found in Mosmann et al. (2004) and Lu et al. (2004). The SQMK test has the following steps:

I. At each comparison, the number of cases $x_i > x_j$ is counted and indicated by n_i , where x_i ($i=1,2,\dots,n$) and x_j ($j=1,2,\dots,n$) are the sequential values in a series, respectively.

II. The test statistic t_i is calculated by

$$t_i = \sum_{j=1}^i n_j \tag{1}$$

III. The mean $E(t)$ and the variance $\text{var}(t_i)$ of the test statistic are calculated by

$$E(t) = \frac{n(n-1)}{4}, \tag{2}$$

$$\text{var}(t_i) = \frac{i(i-1)(2i+5)}{72}. \tag{3}$$

IV. Sequential progressive value can be calculated as

$$u(t) = \frac{t_i - E(t)}{\sqrt{\text{var}(t_i)}}. \tag{4}$$

Similarly, the values of $u'(t)$ are computed backwards, starting from the end of the series.

Results

Sentinel 5P-spatial distribution

Figure 2 shows the presence and incidence of SO_2 in Lephalale, with 2018 showing a more increased gas dispersion. The year 2019 shows a slight increase from the previous year, caused by the high demand for electricity throughout the year and the cold weather during the winter months (Shikwambana et al., 2020). Between 2020 and early 2022, the world was riddled with the COVID-19 pandemic, affecting South Africa and halting many economic activities and movements (Kganyago and Shikwambana, 2020). This affected the production and distribution of electricity, thus decreasing the spatial distribution of SO_2 by the two most productive coal-fired power stations in Limpopo. Although no real column density values in mol/m^2 are presented (the units of measurement for gas column densities), these are replaced by the "minimum" and "maximum values", which essentially show how highly concentrated the municipality of Lephalale, the province of Limpopo and regions nearby are by NO_2 , SO_2 and CO. Based on Figure 2, it is clearly evident that all the years between 2018 and 2022 have had varying concentrations of SO_2 , with 2018 showing more spatial distribution than the other four years preceding it. We anticipate that meteorological parameters like high wind speeds or slightly higher temperatures could be responsible for the higher spatial distribution of SO_2 in 2018.

In Figure 3, 2018 and 2019 depict a fluctuation trend, with a slight difference in their column densities. Similar to SO_2 , the spatial distribution of NO_2 is slightly higher in 2018 than in 2019. Again meteorological parameters are the possible drivers for this. Succeeding these are 2021 and 2022, both having picked up their NO_2 emission rates rapidly after the 2020 lockdown period, where there was little need and usage of electricity

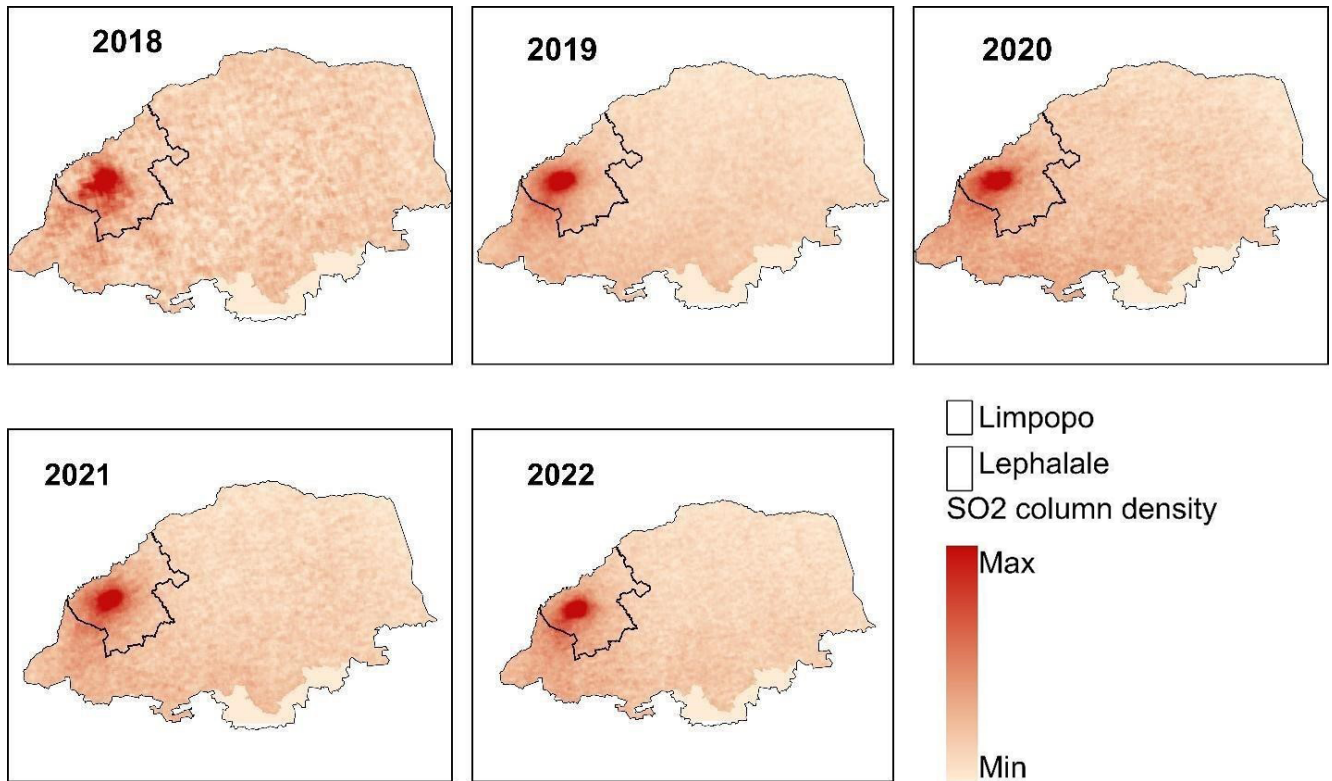


Figure 2: SO₂ column density (mol/m²) trends over Lephalale from 2018-2022 from Sentinel-5P.

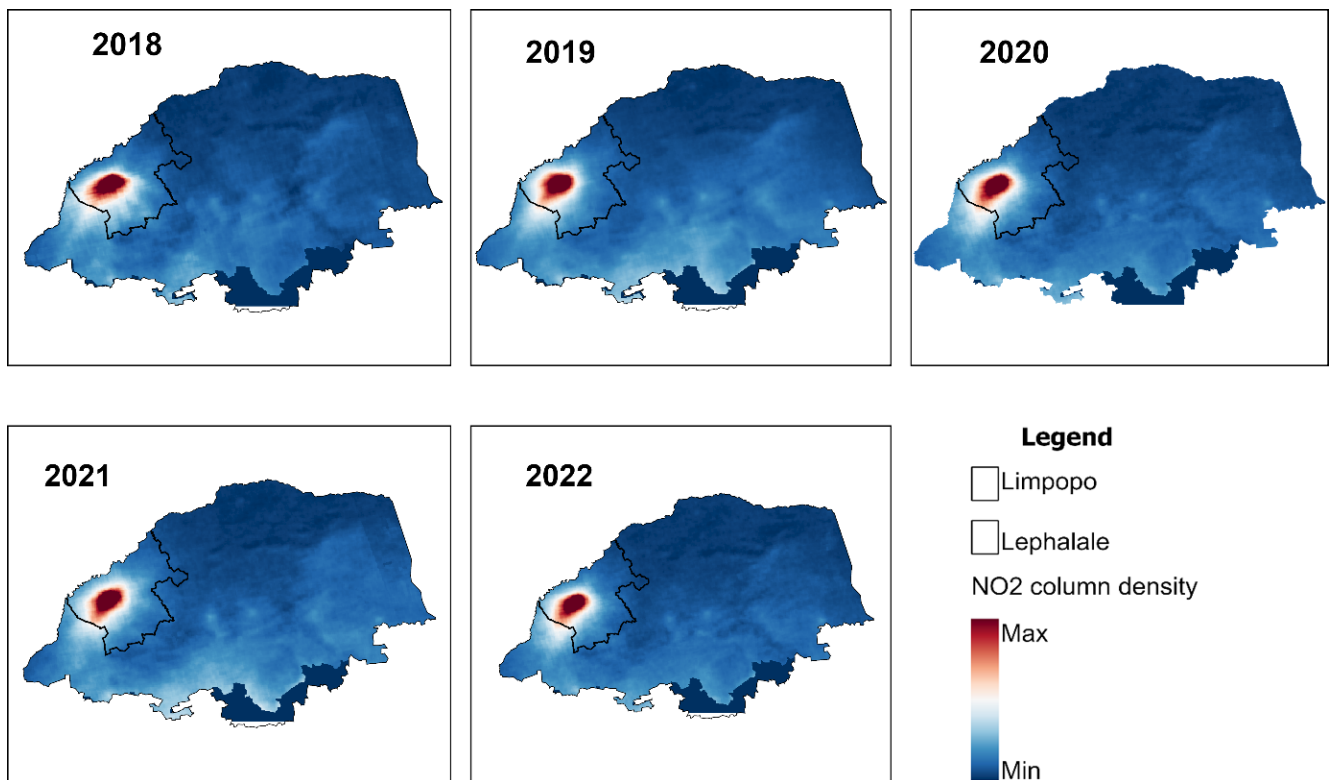


Figure 3: NO₂ column density (mol/m²) trends over Lephalale from 2018-2022 from Sentinel-5P.

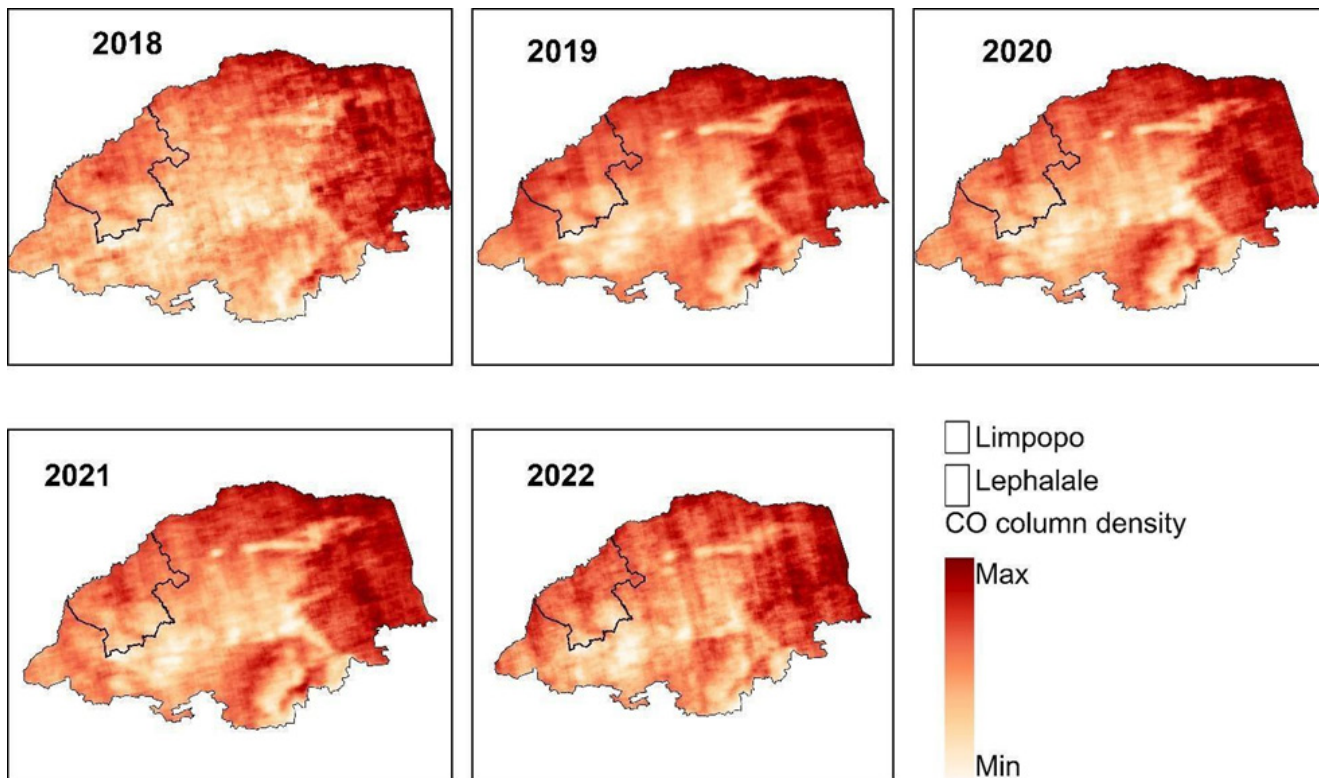


Figure 4: CO column density (mol/m^2) trends over Lephalale from 2018-2022 from Sentinel-5P.

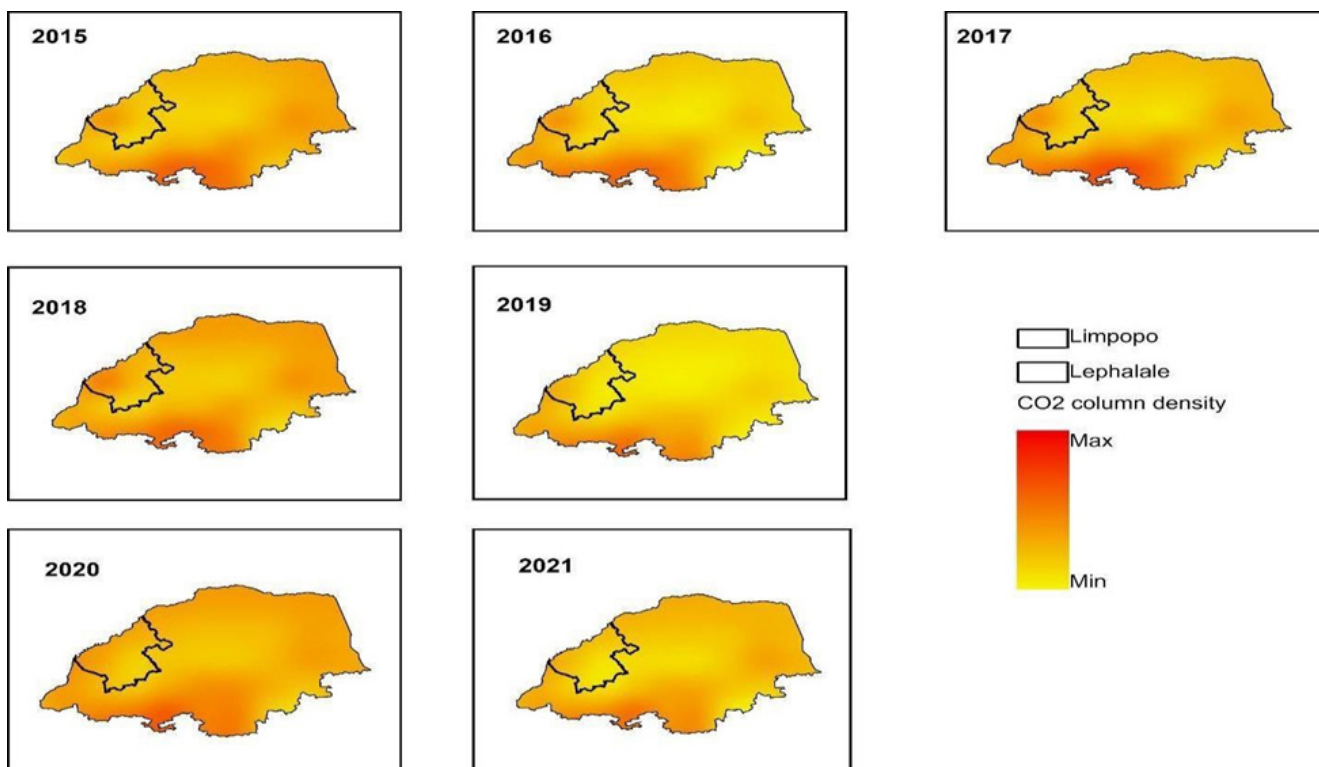


Figure 5: CO_2 column density ($\text{mol CO}_2/\text{mol dry}$) trends over Lephalale from 2015-2021, as observed by GEOS-Chem.

for any economic activity, and traffic was controlled, but more emissions from the burning of biomass agricultural land (Kganyago and Shikwambana, 2020). These are displayed by the column densities, seen in the minimum and maximum descriptions in Figure 3. The year 2018 is seen to have a greater maximum value of NO_2 , followed by 2019. During the same 5-year period, 2020 and 2021 had a lower column density caused by the halting of economic activities due to the global pandemic. However, fossil fuels were still being burnt in households as winters and autumns in Limpopo were harsh (Rapolaki et al., 2021). Overall, compared to the incidence of SO_2 , NO_2 column density decreased due to the possible change to low NO_x coal for less and safer emissions (Shikwambana et al., 2020).

Figure 4 shows the spatial distribution of CO in Lephalale. The years 2020 and 2021 have an equal distribution of CO in and around the study area and its broader location. The years with the highest column density range between $0.0256614 \text{ mol/m}^2$ and $0.0314215 \text{ mol/m}^2$ (not shown in Figure 4). The year 2018 has the least CO column density, followed by 2019 and 2022. A cause of these fluctuations could be due to meteorological factors like wind and temperature. But 2018-2022 had little wind and rain, and 2020-2021 were drought years, these factors might have contributed towards the concentrations and spatial distribution of the CO. Overall, there is no significant presence of CO in Lephalale from the power stations.

Figure 5 shows the CO_2 spatial distribution for the years 2015 to 2022. The years 2015-2018 have the most negligible column density of CO_2 , ranging between $0.00039853 \text{ mol/m}^2$ – $0.00040602 \text{ mol/m}^2$ of the maximum value and $0.000398252 \text{ mol/m}^2$ – $0.000405739 \text{ mol/m}^2$. These could be owing to a stable atmosphere and fewer economic activities, thus affecting the country's GDP. Table 1 also provides evidence that during these years, access to electricity and the amount of CO_2 emissions in South Africa, as provided by the World Bank, were amongst the lowest. From 2019-2021 onwards, there is a steady rise in these emissions, with column density ranging between $0.00040861 \text{ mol/m}^2$ – $0.000413503 \text{ mol/m}^2$ of the maximum and $0.000409091 \text{ mol/m}^2$ – $0.000412969 \text{ mol/m}^2$.

Trend analysis

The Sequential Mann–Kendall (SQMK) trends are presented in Figures 6–9, with the red line representing the progressive series, whereas the blue line represents the retrograde series. The confidence interval for this test is set at $\alpha = 0.05 (\pm 1.96)$. The solid black line represents the upper bound (+1.96), whereas the lower bound (-1.96) is represented by the square dotted black line. The point at which the red and light blue lines intersect indicates an abrupt change and the year in which the change

Table 1: Yearly rates of the percentage of the population with access to electricity and the amount of CO_2 emissions in a thousand tons in South Africa from 2010-2021 (World Bank, 2023).

| Indicator | 2015 | 2016 | 2017 | 2018 | 2019 | 2020 | 2021 |
|--|--------|--------|--------|--------|--------|--------|-------|
| Access to electricity (% of population.) | 85.3 | 83.9 | 84.4 | 84.7 | 85 | 90 | 89.3 |
| CO_2 emissions (kt) | 425063 | 425683 | 435215 | 439645 | 446626 | 393242 | ----- |

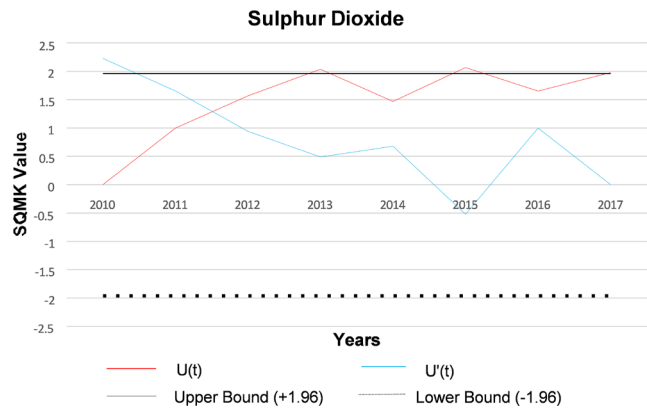


Figure 6: SQMK trends for SO_2 column density in Lephalale between 2010 and 2017.

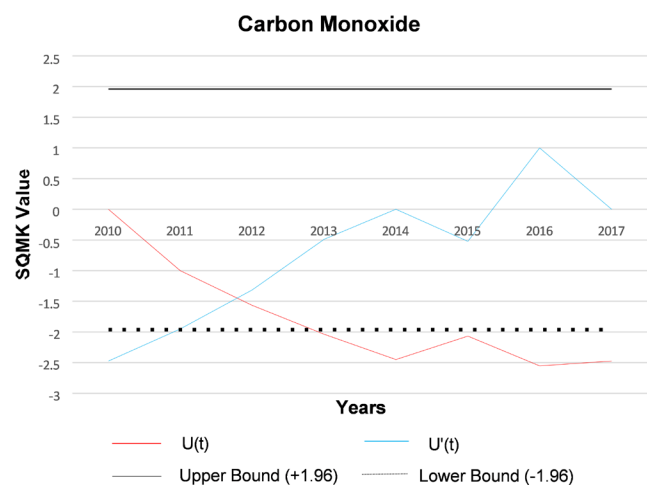


Figure 7: SQMK trends for CO column density in Lephalale between 2010 and 2017.

occurred. A significant trend is observed when the progressive series crosses the lower or upper bounds. In contrast, an insignificant trend is observed when the progressive series is within the upper and lower bounds. The SQMK trends are over the Lephalale region.

Figure 6 shows a trend of the SO_2 column density from 2010 to 2017 in Lephalale. It shows an increasing trend from the later months of 2010 until 2013. From 2014 onwards, there has been a fluctuating trend in the emission of SO_2 : a gradual decline in 2014, a gradual increase in 2015, a decline from then into 2016, and then emissions pick up again into 2017. This steady rise between 2010 and 2013, as having been mentioned before, may strongly have been due to the transfer of emissions between Mpumalanga and Limpopo, affecting the presence of GHGs in both provinces. Fluctuations between 2013 and 2017, wherein

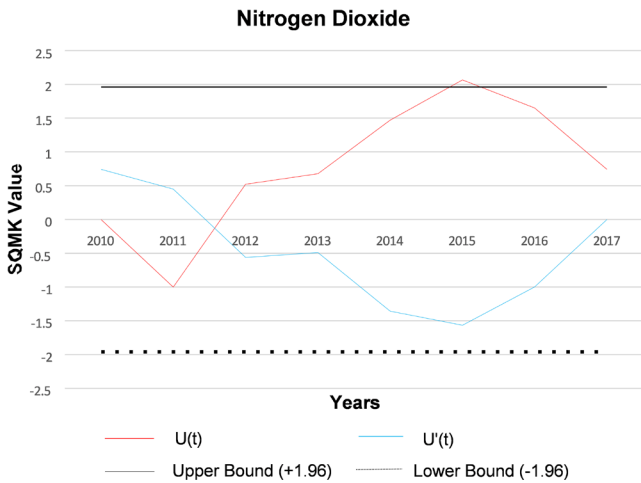


Figure 8: SQMK trends for NO₂ column density in Lephalale between 2010 and 2017.

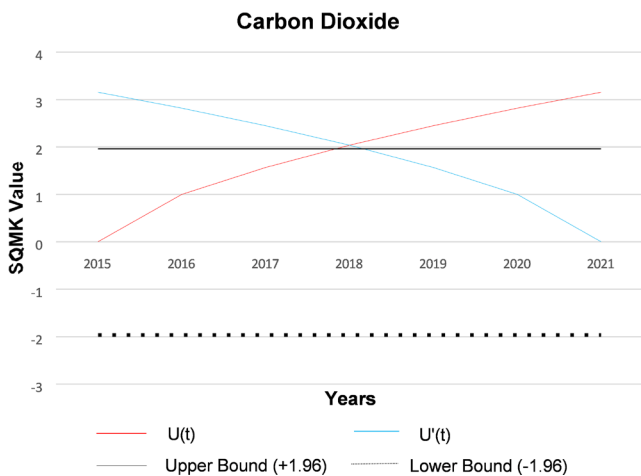


Figure 9: SQMK trends for CO₂ column density in Lephalale between 2010 and 2017.

their column densities and trend lines are still higher than pre-2013, are a result of the full electricity generation of coal-fired power stations and the full operation of coal mines, the Grootegeluk in particular (Shikwambana et al., 2021). Thus, change seems to contradict itself as the $u(t)$ and $u'(t)$ intersect within the two boundary layers, showing insignificant change in the emissions of SO₂, while the years 2013 and 2015 cross over a little beyond the upper boundary layer, which is interpreted as significant change.

The spatial distribution of carbon monoxide, as shown in Figures 5 and 7, is not quite apparent, especially within Lephalale, where the Medupi Power Station is located. However, it is quite noticeable within just Limpopo. That said, a large amount of CO present within the study area is undoubtedly due to the burning of biofuel and biomass more than it is due to fossil fuel burning (Kumar et al., 2011; Shikwambana & Tsoeleng, 2020). As it stands, there is no evident trend change of CO in Lephalale because, even though both progressive and retrograde intersect within boundary layers (insignificant change), only the retrograde series extends beyond the (lower) boundary layer; there is no clear beginning of a trend or significant change in its occurrence.

Figure 7 shows no evident trend change of CO in Lephalale. Even though both progressive and retrograde intersect within boundary layers (insignificant change), only the retrograde series extends beyond the (lower) boundary layer, and there is no clear beginning of a trend or significant change in its occurrence. A large amount of CO present within the study area is undoubtedly due to the burning of biofuel and biomass more than it is due to fossil fuel burning (Kumar et al., 2011; Shikwambana & Tsoeleng, 2020).

Figure 8 shows the column density trend of NO₂ in Lephalale between 2010 and 2017. It shows considerable significant changes in column densities within the study period. Between 2010 and 2011, a significant decline dropped in 2011. The years 2011 to 2012 show a steep increase in the emissions of NO₂, followed by a gradual increase in 2013 and a significant increase between 2013 and 2015. This is followed by a trend of insignificance resulting from coal combustion and agricultural fires, just like SO₂ (Opio et al., 2021). Overall, an insignificant change in the emissions and presence of NO₂ is detected.

The trend in Figure 9 shows CO₂ column densities between 2015 and 2021. The progressive trend line shows a steep increase in the emissions of CO₂ from 2015 to 2016. From there onwards, there will be an even steeper increase in these emissions up until 2021. This is quite interesting because economic activities, including trade and manufacturing, were halted from the end of 2019 until 2021 due to the global pandemic. However, a large portion of this change is due to burning natural gas, electricity production, and burning of biomass and fossil fuels as many people stay home, leading to more household activities than usual. There is an immense significant change in the time-series distribution of CO₂ in Lephalale. The increase in CO₂ is statistically significant from 2018 onwards.

Discussion

GHGs serve as proxies for economic growth and reflect the pace of a country's industrialization (Shikwambana et al., 2021). While this correlation may offer insights into the necessary adjustments for meeting economic objectives, it also highlights a significant risk to public health, particularly with regard to premature morbidity and mortality rates. Limpopo, home to the Medupi and Matimba Power Stations, has seen a rise in energy and transportation industries, contributing to elevated GHG emissions in the province and across South Africa (Selo & Ngole-Jeme, 2022). Air quality data from Lephalale and Limpopo reveal high levels of NO₂, SO₂, CO₂, and CO, underscoring the environmental hazards associated with coal combustion. South Africa is not alone in facing these challenges; other countries experiencing economic growth also struggle with air pollution and its detrimental effects on public health (Mokgoja et al., 2023).

South Africa's reliance on fossil fuels and solid biomass for energy is well-established (Akinbami et al., 2021; Oibileke et al., 2024), driven by a growing population and rapid urbanization, which

increases the demand for energy and industrial development (Nuissl & Siedentop, 2021). A significant portion of emissions comes from the burning of coal for electricity generation, especially in urban and expanding rural areas in South Africa and worldwide (Runsten et al., 2018). For instance, Australia in the Global North generates over 70% of its electricity from coal, while South Africa relies on coal for more than 77% of its electricity needs (Nciphha & Sivakumar, 2022). The key difference lies in population density: while Australia's smaller population enjoys more widespread access to electricity, South Africa faces challenges in equitable distribution, as shown in Table 1.

Although emissions of NO₂, SO₂, CO₂, and CO exceed recently established environmental standards, significant disparities remain in electricity access across South African households (see Table 1). This indicates that efforts to reduce emissions must continue to close the gap in electricity distribution. Despite ongoing discussions on transitioning to green energy for over a decade, South Africa's environmental policies, such as the National Environmental Management: Air Quality Act (NEM: AQA) 39 of 2004, the National Environmental Management Act 107 of 1998, and the National Ambient Air Quality Standards (NAAQS), must be rigorously enforced and strengthened. These measures are crucial to ensure the protection of air quality for all citizens and reduce harmful emissions, ultimately safeguarding the atmosphere and public health (Mokgoja et al., 2023).

Conclusion

This study used remotely sensed data to investigate the spatial and temporal distribution of SO₂, NO₂, CO₂ and CO in Lephalale. This was to illustrate the impact coal-fired power stations have on Limpopo, particularly the Medupi Power Station. The spatial distribution maps showed that the pollutants were due to the operation of the Medupi and Matimba Power Stations. The SQMK trends show that the emissions fluctuate; the year 2010 for SO₂, NO₂ and CO₂ is the beginning of the rise in the atmospheric presence of these gases. Thus, it can be concluded that the air quality in Lephalale is a consequence of these emissions from coal combustion. In addition, if no mitigation measures are taken and strictly followed by coal mines and electricity generators, the lives of the people in and around Lephalale and Limpopo will be severely affected.

Acknowledgements

The author acknowledges the GES-DISC Interactive Online Visualization and Analysis Infra-structure (Giovanni) for providing the MERRA-2, OMI and GEOS-CHEM data. We further thank and acknowledge ESA for the Sentinel-5 P/TROPOMI data.

Data statement

The data used in the study is freely available on the NASA Giovanni data portal.

Conflicts of Interest

The authors declare no conflict of interest.

Funding

No funding was provided for this research.

Ethical approval

The University of the Witwatersrand granted the ethical approval for the research.

Consent to participate

No participants were involved in this research.

Consent to publish

No consent to publish is required for this research.

References

- Akinbami, O.M, Oke, S.R., Bodunrin, M.O. (2021). The state of renewable energy development in South Africa: An overview, *Alexandria Engineering Journal*, 60, 5077-5093. <https://doi.org/10.1016/j.aej.2021.03.065>
- Albers P.N., Wright C.Y., Voyi K.V.V., Mathee A. (2015) Household fuel use and child respiratory ill health in two towns in Mpumalanga, South Africa. *South African Medical Journal*, 105(7), 573-577.
- Arowosegbe O.O., Roosli M., Kunzli N., Saucy A., Adebayo-Ojo T.C., Schwartz J., Kebalepile M., Jeebhay M.F., Dalvie M.A., de Hoogh, K. (2022) Ensemble averaging using remote sensing data to model spatiotemporal PM₁₀ concentrations in sparsely monitored South Africa. *Environmental Pollution*, 310, 1-10.
- Barnes B., Mathee,A., Thomas E., Bruce N. (2009) Household energy, indoor air pollution and child respiratory health in South Africa. *Journal of Energy in Southern Africa*, 20(1), 4-13.
- Boersma K.F., Bucsela E., Brinksma E.J., Gleason J.F. NO₂. In *OMI Algorithm Theoretical Basis Document, OMI Trace Gas Algorithms, ATBOMI-04, Version 2.0*; Chance, K., Ed.; NASA: Washington, DC, USA, 2002; Volume 4, pp. 13–36. Available online: <https://ozoneaq.gsfc.nasa.gov/media/docs/ATBD-OMI-04.pdf> (accessed on 02 August 2023).
- Buchard V., Randles C.A., da Silva A.M., Darmenov A., Colarco P.R., Govindaraju R., Ferrare R., Hair J., Beyersdorf A.J., Ziemba L.D., Yu H. (2017) The MERRA-2 Aerosol Reanalysis, 1980 Onward. Part II: Evaluation and Case Studies. *Journal of Climate*, 30, 6851–6872. <https://doi.org/10.1175/JCLI-D-16-0613.1>
- Bucsela E.J., Celarier E.A., Wenig M.O., Gleason J.F., Veefkind J.P., Boersma K.F., Brinksma E.J. (2006) Algorithm for NO₂ vertical

column retrieval from the ozone monitoring instrument. *IEEE Transactions on Geoscience and Remote Sensing*, 44, 1245–1258. <https://doi.org/10.1109/TGRS.2005.863715>

Duncan B.N., Prados A.I., Lamsal L.N., Liu Y., Streets D.G., Gupta P., Hilsenrath E., Kahn R.A., Nielsen J.E., Beyersdorf A.J., Burton S.P., Fiore A.M., Fishman J., Henze D.K., Hostetler C.A., Krotkov N.A., Lee P., Lin M., Pawson S., Pfister G., Pickering K.E., Pierce R.B., Yoshida Y., Ziemba L.D. (2014) Satellite data of atmospheric pollution for US air quality applications: Examples of applications, summary of data end-user resources, answers to FAQs, and common mistakes to avoid. *Atmospheric Environment*, 94, 647–662. <http://dx.doi.org/10.1016/j.atmosenv.2014.05.061>.

Farzad K., Khorsandi B., Khorsandi M., Bouamra O., Maknoon, R. (2021). Estimating short-term mortality benefits associated with a reduction in tropospheric ozone. *Atmospheric Environment*, 252, 1–8.

Fritz T. M., Eastham S.D., Emmons L.K., Lin H., Lundgren E.W., Goldhaber S., Barrett S.R. H., Jacob D.J. (2022) Implementation and evaluation of the GEOS-Chem chemistry module version 13.1.2 within the Community Earth System Model v2.1. *Geoscientific Model Development*, 15, 8669–8704. <https://doi.org/10.5194/gmd-15-8669-2022>

Gelaro R., McCarty W., Suárez M.J., Todling R., Molod A., Takacs L., Randles C.A., Darmenov A., Bosilovich M.G., Reichle R., Wargan K., Coy L., Cullather R., Draper C., Akella S., Buchard V., Conaty A., da Silva A.M., Gu W., Kim G., Koster R., Lucchesi R., Merkova D., Nielsen J.E., Partyka G., Pawson S., Putman W., Rienecker M., Schubert S.D., Sienkiewicz M., Zhao B. (2017) The Modern-Era Retrospective Analysis for Research and Applications, Version 2 (MERRA-2). *Journal of Climate*, 30, 5419–5454. <https://doi.org/10.1175/JCLI-D-16-0758.1>

Gupta P., Christopher S.A., Wang J., Gehrig R., Lee Y., Kumar, N. (2015) Satellite remote sensing of particulate matter and air quality assessment over global cities. *Atmospheric Environment*, 40(30), 5880–5892.

Kganyayo M., Shikwambana, L. (2020). Assessment of the characteristics of recent major wildfires in the USA, Australia and Brazil in 2018–2019 using multi-source satellite products. *Remote Sensing*, 12(11). <https://doi.org/10.3390/rs12111803>

Kganyayo M., Shikwambana, L. (2021). Did COVID-19 Lockdown Regulations have an impact on Biomass Burning Emissions in Sub-Saharan Africa? *Aerosol Air Quality Research*, 21(4). <https://doi.org/10.4209/aaqr.2020.07.0470>.

Jiang K., Fu B., Luo Z., Xiong R., Men Y., Shen H., Li B., Shen G., Tao S. (2022). Attributed radiative forcing of air pollutants from biomass and fossil burning emissions. *Environmental Pollution*, 306, 1–9.

Kumar R., Naja M., Pfister, G.G., Barth M.C., Brasseur G.P. (2013) Source attribution of carbon monoxide in India and

surroundings during wintertime. *Journal of Geophysical Research: Atmospheres*, 18, 1981–1995. <https://doi.org/10.1002/jgrd.50134>.

Lelieveld J., Klingmüller K., Pozzer A., Ramanathan V. (2019). Effects of fossil fuel and total anthropogenic emission removal on public health and climate. *Earth, Atmospheric, and Planetary Sciences*, 116(15), 7192–7197. <https://doi.org/10.1037/pnas1819981116>.

Levelt P.F., Hilsenrath E., Leppelmeier G.W., van den Oord G.H.J., Bhartia K., Tamminen J., de Haan J.F., Veefkind J.P. (2006) Science objectives of the ozone monitoring instrument. *IEEE Transactions on Geoscience and Remote Sensing*, 44, 1199–1208. <https://doi.org/10.1109/TGRS.2006.872336>.

Levelt P.F., Joiner J., Tamminen J., Veefkind J.P., Bhartia P.K., Stein Zweers D.C., Duncan B.N., Streets D.G., Eskes H., van der Ronald A.; et al. (2018) The Ozone Monitoring Instrument: Overview of 14 years in space. *Atmospheric Chemistry and Physics*, 18, 5699–5745. <https://doi.org/10.5194/acp-18-5699-2018>.

Lu A., He Y., Zhang Z., Pang H., Gu, J. (2004). Regional Structure of Global Warming across China during the Twentieth Century. *Climate Research*, 27, 189–195. doi:10.3354/cr027189

Marcatelli M. (2020). Medupi power station and the water-energy nexus in South Africa. *Transformation: Critical Perspectives on Southern Africa*, 102, 1–26. <https://doi.org/10.1353/trn.2020.0000>

Miatselskaya N., Bril A., Chaikovskiy A., Miskevich A., Milinevsky G., Yukhymchuk Y. (2022) Spatio-Temporal Optimal Interpolation of Aerosol Optical Depth Observations Using a Chemical Transport Model. *Environmental Sciences Proceedings*. 19(1), 7. <https://doi.org/10.3390/ecas2022-12797>

Mokgoja B., Mhangara P., Shikwambana L. (2023) Assessing the Impacts of COVID-19 on SO₂, NO₂, and CO Trends in Durban Using TROPOMI, AIRS, OMI, and MERRA-2 Data. *Atmosphere*, 14(8). <https://doi.org/10.3390/atmos14081304>

Mosmann V., Castro A., Fraile R., Dessens J., Sanchez J.L. (2004) Detection of statistically significant trends in the summer precipitation of mainland Spain. *Atmospheric Research*, 70, 43–53.

Mutezo G., Mulopo J. (2021). A review of Africa's transition from fossil fuels to renewable energy using circular economy principles. *Renewable and Sustainable Energy Reviews*, 197, 1–15.

Muthige S.M. (2013). *Ambient air quality impacts of a coal-fired power stations in Lephalale area* [Master's dissertation]. University of the Witwatersrand, South Africa.

Ncipha X.G., Sivakumar, V. (2022) The first national scale spatial and temporal analysis of surface CO₂ over South Africa utilising satellite retrievals. *South African Geographical Journal*, 104(2), 137–154. <https://doi.org/10.1080/03736245.2021.1934093>

- Nuissl, H., Siedentop, S. (2021). Urbanisation and Land Use Change. In: Weith, T., Barkmann, T., Gaasch, N., Rogga, S., Strauß, C., Zscheischler, J. (eds) Sustainable Land Management in a European Context. Human-Environment Interactions, vol 8. Springer, Cham. https://doi.org/10.1007/978-3-030-50841-8_5
- Obileke K, Mukumba P, Lesala ME (2024). Advancement of Bioenergy Technology in South Africa. *Energies*, 17(15):3823. <https://doi.org/10.3390/en17153823>
- Opio R., Mugume I., Natakumba-Nabende, J. (2021) Understanding the Trend of NO₂, SO₂ and CO over East Africa from 2005 to 2020. *Atmosphere*, 12(10), 1-15. <https://doi.org/10.3390/atmos12101283>.
- Peel M.C., Finlayson B.L., McMahon T.A. (2007). Updated world map of the Koppen-Geiger climate classification. *Hydrology and Earth System Sciences*, 11, 1633-1644, www.hydrol-earth-syst-sci.net/11/1633/2007.
- Randles C.A., da Silva A.M., Buchard V., Colarco P.R., Darmenov A., Govindaraju R., Smirnov A., Holben B., Ferrare R., Hair J., Shinozuka Y., Flynn C.J. (2017) The MERRA-2 Aerosol Reanalysis, 1980 Onward. Part I: System Description and Data Assimilation Evaluation. *Journal of Climate*, 30, 6823-6850. <https://doi.org/10.1175/JCLI-D-16-0609.1>
- Rapolaki R.S., Blamey R.C., Hermes J.C., Reason CJC (2021) Moisture sources and transport during an extreme rainfall event over the Limpopo River Basin, southern Africa. *Atmospheric Research*, 264, 1-52.
- Runsten S., Nerini F.F., Tait, L. (2018) Energy provision in South African informal urban Settlements – A multi-criteria sustainability analysis. *Energy Strategy Reviews*, 19, 76-84. <https://doi.org/10.1016/j.esr.2017.12.004>.
- Shamuyarira K.K., Gumbo, JR (2014) Assessment of Heavy Metals in Municipal Sewage Sludge: A Case Study of Limpopo Province, South Africa. *International Journal of Environmental Research and Public Health*, 11, 2569-2579. <https://doi.org/10.3390/ijerph110302569>
- Seloa P., Ngole-Jeme V. (2022) Community Perceptions on Environmental and Social Impacts of Mining in Limpopo South Africa and the Implications on Corporate Social Responsibility. *Journal of Integrative Environmental Sciences*, 19(1), 189-207.
- Shami S., Rangjar B., Bian J., Azar M.K., Moghimi A., Amani M., Naboureh A. (2022). Trends of CO and NO₂ Pollutants in Iran during COVID-19 Pandemic Using Timeseries Sentinel-5 Images in Google Earth Engine. *Pollutants*, 2(2), 156-171.
- Shikwambana L., Sivakumar V. (2018) Global distribution of aerosol optical depth in 2015 using CALIPSO level 3 data. *Journal of Atmospheric and Solar-Terrestrial Physics*, 173, 150-159.
- Shikwambana L., Tsoeleng L.T. (2020) Impacts of population growth and land use on air quality: A case study of Tshwane, Rustenburg and Emalahleni, South Africa. *South African Geographical Journal*, 102(2), 209-222.
- Shikwambana L., Mhangara P., Mbatha N. (2020) Trend analysis and first-time observations of sulphur dioxide and nitrogen dioxide in South Africa using TROPOMI/Sentinel-5 P data. *International Journal of Applied Earth Observation and Geoinformation*, 91, 1-13.
- Sneyers R. (1991) On the Statistical Analysis of Series of Observations; World Meteorological Organization (WMO): Geneva, Switzerland.
- Theys N., Hedelt, T. De Smedt I., Lerot C., Yu H., Vlietinck J., Pedergnana M., Arellano S., Galle B., Fernandez D., Carlito C.J.M., Barrington C., Taisne B., Delgado-Granados H., Loyola D., Van Rozendael M. (2019). Global monitoring of volcanic SO₂ degassing with unprecedented resolution from TROPOMI onboard Sentinel-5 Precursor. *Scientific Reports*, 9 (2643). <https://doi.org/10.1038/s41598-019-39279-y>.
- Tilstra L.G., de Graaf M., Wang P., Stammes P. (2020) In-orbit Earth reflectance validation of TROPOMI on board the Sentinel-5 Precursor satellite. *Atmospheric Measurement Techniques*, 13, 4479–4497. <https://doi.org/10.5194/amt-13-4479-2020>
- Verhoelst T., Compornolle S., Pinardi G., Lambert J.-C., Eskes H. J., Eichmann K.-U., Fjæraa A. M., Granville J., Niemeijer S., Cede A., Tiefengraber M., Hendrick F., Pazmiño A., Bais A., Bazureau A., Boersma K. F., Bogner K., Dehn A., Donner S., Elokhov A., Gebetsberger M., Goutail F., Grutter de la Mora M., Gruzdev A., Gratsea M., Hansen, G.H., Irie H., Jepsen N., Kanaya Y., Karagiozidis D., Kivi, R., Kreher K., Levelt P. F., Liu C., Müller M., Navarro Comas M., Piters A.J.M., Pommereau J.-P., Portafaix T., Prados-Roman C., Puentedura O., Querel R., Remmers J., Richter A., Rimmer J., Rivera Cárdenas C., Saavedra de Miguel L., Sinyakov V. P., Stremme W., Strong K., Van Roozendael M., Veeffkind J.P., Wagner T., Wittrock F., Yela González M., & Zehner C. (2021). Ground-based validation of the Copernicus Sentinel-5P TROPOMI NO₂ measurements with the NDACC ZSL-DOAS, MAX-DOAS and Pandora global networks. *Atmospheric Measurement Techniques*, 14, 481–510. <https://doi.org/10.5194/amt-14-481-2021>
- Wernecke, B., Naidoo, N.P., Wright, C.Y. (2023). Establishing a baseline of published air pollution and health research studies in the Waterberg-Bojanala Priority Area. *Clean Air Journal*, 33. <https://doi.org/10.17159/caj/2023/33/1.14887>
- Winning A. (2021). Africa's top emitter seeks \$10 bln for shift from coal. *Reuters*, <https://www.reuters.com/business/environment/africas-top-emitter-seeks-10-blshift-coal-2021-06-30/> (Accessed on 27 August 2023)
- World Bank, 2023. <https://data.worldbank.org/indicator/EN.ATM.CO2E.KT> (Accessed 15 October 2023).